McIntosh, L. P., & Dahlquist, F. W. (1990) *Q. Rev. Biophys. 23*, 1–38.
Morris, G. A., & Freeman, R. (1979) *J. Am. Chem. Soc. 101*, 760–762.
Oefner, C., D'Arcy, A., & Winkler, F. K. (1988) *Eur. J. Biochem. 174*, 377–385.
Piantini, U., Sørensen, O. W., & Ernst, R. R. (1982) *J. Am. Chem. Soc. 104*, 6800–6801.
Prendergast, N. J., Delcamp, T. J., Smith, P. L., & Freisheim, J. H. (1988) *Biochemistry 27*, 3663–3671.
Reddy, A. V., Behnke, W. D., & Freisheim, J. H. (1978) *Biochim. Biophys. Acta 533*, 415–427.
Shaka, A. J., Barker, P. B., & Freeman, R. (1985) *J. Magn. Reson. 64*, 547–552.
Stammers, D. K., Champness, J. N., Beddell, C. R., Dann, J. G., Eliopoulos, E., Geddes, A. J., Ogg, D., & North, A. C. T. (1987) *FEBS Lett. 218*, 178–184.
Stockman, B. J., Nirmala, N. R., Wagner, G., Delcamp, T. J., DeYarman, M. T., & Freisheim, J. H. (1991) *FEBS Lett. 283*, 267–269.
Wagner, G. (1990) *Prog. Nucl. Magn. Reson. Spectrosc. 22*, 101–139.
Wagner, G., Hyberts, S. G., & Havel, T. F. (1991) *Annu. Rev. Biophys. Biomol. Struct.* (in press).
Wüthrich, K. (1986) *NMR of Proteins and Nucleic Acids*, Wiley, New York.
Zuiderweg, E. R. P., & Fesik, S. W. (1989) *Biochemistry 28*, 2387–2391.
Zuiderweg, E. R. P., McIntosh, L. P., Dahlquist, F. W., & Fesik, S. W. (1990) *J. Magn. Reson. 86*, 210–216.

^1H and ^{15}N NMR Characterization of Free and Bound States of an Amphiphilic Peptide Interacting with Calmodulin†

Bénédicte Prêcheur,‡ Hélène Munier,§ Joël Mispelter,‖ Octavian Bârzu,§ and Constantin T. Craescu*,‡

Institut National de la Santé et de la Recherche Médicale U91 and Centre National de la Recherche Scientifique URA 607, Hôpital Henri Mondor, 94010 Créteil, France, Unité de Biochimie des Régulations Cellulaires, URA 1129, Institut Pasteur, Paris, France, and Institut National de la Santé et de la Recherche Médicale U219, Institut Curie, Orsay, France

Received July 24, 1991; Revised Manuscript Received September 26, 1991

ABSTRACT: A peptide of 17 amino acid residues Ac-L-K-W-K-K-L-L-K-L-L-K-K-L-L-K-L-G-NH_2, designed to form an amphiphilic basic α-helix [DeGrado, W. F., Prendergast, F. G., Wolfe, H. R., Jr., & Cox, J. A. (1985) *J. Cell. Biochem. 29*, 83–93], was labeled with ^{15}N at positions 1, 7, 9, and 10. Homo- and heteronuclear NMR techniques were used to characterize the conformational changes of the peptide when it binds to calmodulin in the presence of Ca^{2+} ions. The spectrum of the free peptide in aqueous solution at pH 6.3 and 298 K was completely assigned by a combined application of several two-dimensional proton NMR methods. Analysis of the short- and medium-range NOE connectivities and of the secondary chemical shifts indicated that the peptide populates, to a significant extent, an α-helix conformational state, in agreement with circular dichroism measurements under similar physicochemical conditions. ^{15}N-edited 1D spectra and $^{15}N(\omega_2)$-half-filtered two-dimensional NMR experiments on the peptide in a 1:1 complex with calmodulin allowed assignment of half of the amide proton resonances and three $C_\alpha H$ resonances of the bound peptide. The observed NOE connectivities between the peptide backbone protons are indicative of a stable helical secondary structure spanning at least the fragment L1–K11. The equilibrium and dynamic NMR parameters of the bound peptide are discussed in terms of a molecular interaction model.

Calmodulin (CaM)[1] is one of the major Ca^{2+}-dependent regulators of intracellular metabolism in eukaryotes. In the presence of Ca^{2+} ions, CaM undergoes conformational changes and can modulate the activities of a wide variety of enzymes such as protein kinases, cyclases, NAD kinases, phosphodiesterases, and calcium pumps (Cohen & Klee, 1988). Limited proteolysis and site-directed mutagenesis allowed identification of the CaM-binding sequences in several target enzymes. Despite little similarity between different CaM-binding sequences, all have in common a high proportion of basic and hydrophobic side chains, an almost complete lack of acidic side chains and a periodicity (with a three to four residue period) of hydrophobic residues along the sequence which suggests a propensity for amphiphilic α-helix secondary structure (Cox et al., 1985).

Synthetic peptides of 12–33 amino acid residues, modeled on the CaM-binding sites of various enzymes, have been shown to bind CaM in a Ca^{2+}-dependent manner. The dissociation constant of these peptides was close, if not identical to, that measured for the intact proteins, suggesting that the molecular features of the CaM/target enzyme interaction are basically reproduced in the model system. A variety of physicochemical techniques, including isotope labeling (DeGrado et al., 1985), fluorescence (Cox et al., 1985; DeGrado et al., 1985), CD (Cox et al., 1985; O'Neil et al., 1987; Garone & Steiner, 1990), X-ray and neutron diffraction (Trewhella et al., 1990), and NMR (Seeholzer et al., 1986; Klevit et al., 1985), were used

† This work was supported by grants from Centre National de la Recherche Scientifique (URA 607 and URA 1129).
* To whom correspondence should be addressed.
‡ Hôpital Henri Mondor.
§ Institut Pasteur.
‖ Institut Curie.

[1] Abbreviations: CaM, calmodulin; CD, circular dichroism; NMR, nuclear magnetic resonance; 2D, two dimensional; COSY, *J*-correlated spectroscopy; RCOSY, relayed correlated spectroscopy; TOCSY, total correlation spectroscopy; NOESY, nuclear Overhauser enhancement spectroscopy.

0006-2960/92/0431-229$03.00/0

to characterize the complexes formed by CaM with various peptides. The collected information, especially the above-mentioned prerequisite for a hydrophobic periodicity, led DeGrado et al., (1985) to design a 17 amino acid basic amphiphilic α-helix peptide [that will be called Baa17 in the following, an acronym recently proposed by the authors (O'Neil & DeGrado, 1990)]. Although unrelated to any other known CaM-binding sequence, Baa17 interacted strongly with CaM (the dissociation constant K_d = 0.2 nM) in a 1:1 stoichiometry. A number of spectroscopic (CD, fluorescence), enzymatic, and chemical methods were used (DeGrado et al., 1985; O'Neil et al., 1987, 1989; O'Neil & DeGrado, 1989) for the conformational and topological characterization of the complex. Despite this effort, some aspects concerning the interaction mechanism are still unclear or under debate: the need for preexistence of a definite conformation of the peptide; structural changes in the protein and peptide structure upon complexation; the nature and the geometry of the intermolecular interactions, etc.

NMR spectroscopy is particularly suitable for studying the structure and dynamics of biomolecules and their interactions under solution conditions which mimic the physiological media (Wüthrich, 1986). Use of ^{13}C and/or ^{15}N labeling combined with heteronuclear two- and three-dimensional magnetic resonance methods (Otting & Wüthrich, 1990; Fesik & Zuiderweg, 1990) enables simplification of the spectra of complex systems by editing subspectra corresponding to chosen labeled components. We decided to apply this direct and nonperturbative approach to study the conformational changes accompanying binding of Baa17 to CaM. With the aim of doing this, we incorporated ^{15}N-labeled Leu residues in positions 1, 7, 9, and 10 of the Baa17 sequence. The proton resonances in the spectrum of the free peptide were assigned by conventional homonuclear 2D methods, and the elements of secondary structure were determined from short- and medium-range dipolar interactions, chemical shift distribution, and temperature coefficients for amide protons. Analysis of these parameters indicated the presence of a significant proportion of helical conformation, in rapid equilibrium with the unfolded extended conformation. The 1:1 complex between CaM and the peptide was then studied by 1D and 2D ^{15}N-filtered proton-detected spectroscopy. The results showed that the conformational equilibrium is now largely shifted toward the helical structure and provided a number of structural and dynamical characteristics of the bound state.

Materials and Methods

Chemicals. Deuterated water (99.98%) was obtained from the Commissariat â l'Energie Atomique (France) and 2,2,2-trifluoroethanol from Aldrich. Hog brain calmodulin, yeast alcohol dehydrogenase, and NAD^+ came from Boehringer Mannheim and sodium α-ketoisocaproate was provided by Sigma. ^{15}N-labeled L-leucine was obtained essentially by the same method used to prepare L-[^{15}N]alanine (Mocanu et al., 1982). The coupled enzymatic synthesis system contained 60 mM of both $^{15}NH_4Cl$ (MSD Isotopes, Montreal, Canada, 99% isotopic enrichment) and α-ketoisocaproate, catalytic (0.5 mM) amounts of NAD^+ and an excess of ethanol (400 mM), alcohol dehydrogenase (5000 units), and leucine dehydrogenase (600 units) in a total volume of 400 mL. The last enzyme was used as a crude preparation which follows a heating step (Nagata et al., 1988). Details concerning synthesis of L-[^{15}N]leucine will be published elsewhere.

Peptide Synthesis. The 17 amino acid peptide Ac-L-K-W-K-K-L-L-K-L-L-K-K-L-L-K-L-G-NH_2 was synthesized by a solid-phase method on chloromethyl-substituted polystyrene resin cross-linked by 1% divinyl benzene. The residues were added using the symmetrical anhydride coupling method (Hancock et al., 1973). The four Leu residues in boldface type are ^{15}N-labeled. The purity of the synthetic peptide was assessed by HPLC and amino acid analysis after 24 h of digestion at 383 K in 6 M HCl.

^1H NMR Samples. The peptide sample, at a concentration of 6 mM, was pepared in a deuterated phosphate buffer (10 mM), pH 6.3, 95% ^1H_2O/5% ^2H_2O. The calmodulin solution (at about 0.5 mM) was obtained by resuspension of the lyophilized powder in an aqueous buffer containing 20 mM Bis-Tris, 100 mM KCl, 6 mM $CaCl_2$, and 5% ^2H_2O, pH 6.3. The solution was extensively dialyzed against the same buffer at 277 K. The peptide, prepared in the same buffer, was then slowly added to the protein solution and the complex (1:1 stoichiometry) was concentrated up to 1.5 mM using Centrisart I tubes (Sartorius, France).

NMR Methods. The NMR spectra were obtained on Bruker AM400 and AM600 spectrometers. Standard homonuclear methods were used to obtain pure absorption DQF-COSY (Rance et al., 1983), RCOSY (mixing period 36 ms) (Eich et al., 1982), phase-sensitive NOESY (Jeener et al., 1979), and z-filtered TOCSY (100-ms mixing time) (Rance, 1987) spectra. The water resonance was suppressed by a low-power selective irradiation during the relaxation delay and also during the mixing time for NOESY spectra. Different mixing times were used for the free peptide (150 and 300 ms) and for the peptide/protein complex (100 and 250 ms), and the spectra were compared to assess the extent of spin diffusion. Usually, 500 experiments were done with 64–96 scans and 2K complex points each.

The proton-detected ^{15}N-filtered 1D and $^{15}N(\omega_2)$-half-filtered 2D spectra were obtained using a reverse-detection probe of the Bruker AM600 spectrometer. The pulse sequences were those firstly proposed by Bax et al. (1983) with slight modifications to improve the water suppression and preset the phase correction (M. Rance, personal communication). In the case of the peptide/CaM complex, we used 30 ms of spin lock for TOCSY spectrum and 100 or 250 ms of mixing time for NOESY spectra.

Data processing was performed with the FTNMR and FELIX softwares (Hare Research, Inc.) running on a SUN 3/160 or a Personal Iris 4D25. Time data were multiplied by sine-bell window functions shifted by $\pi/10$ in the t_2 dimension and by $\pi/4$ in the t_1 dimension. The data were zero-filled in both dimensions to give a final frequency matrix of 4K × 4K real points. Chemical shifts were referenced with respect to the *N*-acetyl methyl group which constantly resonates at 2.06 ppm from 2,2-dimethyl-2-silapentane-5-sulfonate (DSS).

Circular Dichroism. CD spectra were recorded on a Jobin Yvon Dichograph Mark V in 0.2-cm path length cells. The peptide solution was usually 50 μM in 20 mM Bis-Tris buffer in the presence of various concentrations of 2,2,2-trifluoroethanol. The peptide concentration was accurately determined by its Trp optical absorption at 280 nm.

Results

Spectroscopic Studies of the Free Peptide

Resonance Assignment. The use of NMR spectroscopy for the determination of secondary and tertiary structure of peptides and proteins requires first the assignment of each resonance to its corresponding proton in the molecule. Assignment of the ^1H NMR spectrum of the free peptide was made using the standard procedure proposed by Wüthrich (1986). The first step was the identification of spin systems

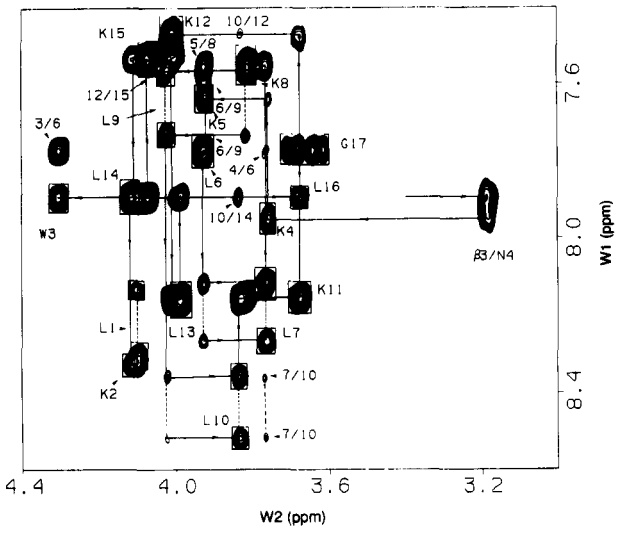

FIGURE 1: Portion of a 600-MHz NOESY spectrum of Baa17 (mixing time 150 ms) in a deuterated phosphate buffer (10 mM), 95% ^1H_2O/5% ^2H_2O, at 298 K and pH 6.3. The region shown contains the $d_{N\alpha}(i,i)$ and the $d_{\alpha N}(i,i+1)$ connectivities and illustrates the sequence-specific assignment. The squares indicate the position of COSY-type connectivities. The NOE cross-peaks which arose from medium-range connectivities $\alpha N(i,i+2)$ and $\alpha N(i,i+3)$ are indicated in the figure.

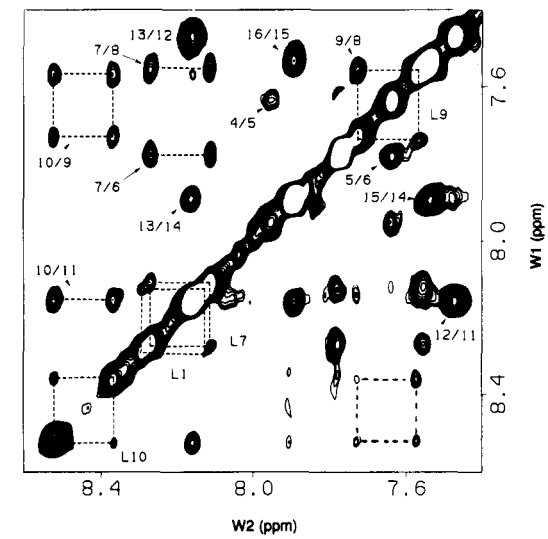

FIGURE 2: Portion of a 600-MHz NOESY spectrum of Baa17 showing the amide/amide cross-peaks. The experimental conditions are the same as in Figure 1.

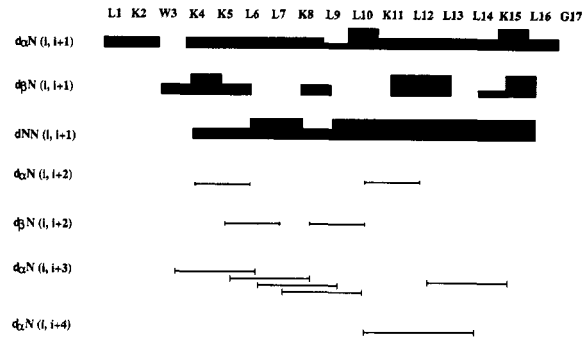

FIGURE 3: Diagrammatic representation qualitatively showing the interresidue NOE connectivities (mixing time 150 ms) along the sequence of Baa17. The thickness of the lines representing the sequential connectivities is proportional to the cross-peak intensity, evaluated by volume integration.

corresponding to the different amino acid types in the peptide sequence using the 2QF-COSY, RCOSY, and TOCSY spectra acquired under the same physicochemical conditions (pH 6.3, 298 K). Despite a highly degenerate primary structure (eight Leu, seven Lys) the NH and $C_\alpha H$ regions were sufficiently dispersed to permit a relatively easy identification of individual cross-peaks. The single Gly and the aromatic Trp spin systems were easily identified by their characteristic cross-peaks. Also, the amide protons of the four labeled Leu residues were readily determined due to the split cross-peaks at amide ω_2 frequencies (the $^{15}N/H$ spin–spin coupling is 92 Hz).

The second step was the assignment of the identified spin systems to the corresponding amino acids in the peptide structure. This was mainly based on the $C_\alpha H/NH(i,i+1)$ NOE sequential connectivities which, together with the intraresidue $C_\alpha H/NH(i,i)$ through-bond correlation connectivities, created an almost continuous pattern of sequential connectivities. The presence of paired cross-peaks corresponding to the four labeled Leu residues in known positions was very helpful in initiating and confirming the assignment. The procedure is illustrated in Figure 1, which shows the fingerprint region of the NOESY spectrum. The string of sequential connectivities was interrupted between W3 and K4 but the presence of a cross-peak between $C_\beta H_2$ of W3 and NH of the K4 permitted continuation of the assignment. Some of the peaks indicated in the figure (i.e., 5/8, 6/9, and 12/15) were better defined in the symmetric part of the spectrum where the resolution in the amide dimension is greater. The assignment results are summarized in Table I.

Secondary Structure. It is commonly accepted that small linear peptides in aqueous solution do not have a unique spatial conformation but sample a number of different conformational states (Wright et al., 1988). However, the presence of regular secondary structure could be shown, in some cases, using a number of NMR parameters. The most powerful are the short- and medium-range NOE connectivities which give intramolecular distance information: their build-up rate is proportional to the inverse sixth power of the interproton distance. Figure 2 shows the amide/amide region of the NOESY spectrum (mixing time 150 ms) of the free peptide at 298 K. A large number of strong sequential $d_{NN}(i,i+1)$ NOEs could be readily observed. Figure 1 also illustrates the presence of nonambiguous medium-range connectivities $d_{\alpha N}(i,i+2)$ and $d_{\alpha N}(i,i+3)$. The summary of the most important short- and medium-range interresidue dipolar connectivities observed for the free peptide is pictured in Figure 3. Most striking is the continuous series of d_{NN} NOE cross-peaks from K4 to L16 whose intensities are generally larger than for the corresponding $d_{\alpha N}(i,i+1)$. A significant number of medium-range dipolar connectivities involving backbone and side-chain protons were observed in the region delimited by K2 and K15. All these elements indicate that the free Baa17 populates an α-helix conformational state (Wüthrich et al., 1984). The helical secondary structure spans about 75% of the peptide length. Observation of $d_{\alpha N}(i,i+1)$ NOEs (Figure 3) which are characteristic of extended conformations means that the helical structures are in rapid exchange with unfolded conformations.

The distribution of the secondary shifts (the difference between the random coil and observed chemical shifts) of the backbone protons along the sequence may also be indicative of regular secondary structure. It has been recently shown that there is a significant difference between the C_α and amide proton chemical shifts of the residues localized in helical, β-sheet, and random-coil structures (Veitch et al., 1988; Szilagyi & Jardetzky, 1989). The chemical shift values ob-

Table I: Chemical Shifts and Temperature Coefficients of Amide Protons for Baa17 in 10 mM Phosphate Buffer, pH 6.3, 95% ^1H_2O/5% ^2H_2O, at 298 K[a]

residue	chemical shift (ppm) NH	$C_\alpha H$	$C_\beta H$	other	$-\Delta\delta/\Delta K$ (10^{-3} ppm/K)
L1	8.22 (8.5)	4.10 (3.93)	1.50	γH 1.37 δCH_3 0.76, 0.82	8.4
K2	8.33 (9.13)	4.12	1.61	γCH_2 1.17, 1.12; δCH_2 1.47; εCH_2 2.78	4.8
W3	7.90	4.30	3.19	2 H 7.23; 4 H 7.30; 5 H 6.75; 6 H 6.94; 7 H 7.33; NH 10.24	3.2
K4	7.95	3.76	1.75	γCH_2 1.34, 1.20; δCH_2 1.60; εCH_2 2.90	5.6
K5	7.63	3.92	1.83, 1.74	γCH_2 1.47, 1.30; δCH_2 1.58; εCH_2 2.85	5.6
L6	7.77 (7.62)	3.93	1.75	γH 1.52; δCH_3 0.77, 0.70	5.2
L7	8.19 (8.32)	3.77	1.55	γH 1.51; δCH_3 0.76, 0.72	0.5
K8	7.55 (7.82)	3.81	1.83	γCH_2 1.51, 1.31; δCH_2 1.60; εCH_2 2.88	0.6
L9	7.64 (7.26)	4.02 (3.75)	1.75	γH 1.60; δCH_3 0.82, 0.78	0.5
L10	8.44 (8.58)	3.83 (3.77)	1.71, 1.75	γH 1.39; δCH_3 0.71, 0.74	4
K11	8.16 (8.25)	3.68	1.72, 1.67	γCH_2 1.39, 1.09; δCH_2 1.47; εCH_2 2.92	2.4
K12	7.47	4.01	1.88	γCH_2 1.50, 1.34; δCH_2 1.59; εCH_2 2.86	0.5
L13	8.16	3.99	1.70	γH 1.47; δCH_3 0.70, 0.73	2.4
L14	7.89	4.11	1.68	γH 1.68; δCH_3 0.69, 0.74	3.6
K15	7.53	4.07	1.87	γCH_2 1.41, 1.35; δCH_2 1.61; εCH_2 2.94	0.5
L16	7.89	3.68	1.59	γH 1.58; δCH_3 0.76, 0.69	3.6
G17	7.77	3.69, 3.62			6

[a] In parentheses are given the chemical shifts of some amide and C_α protons from the bound peptide.

served for C_α and amide protons in Baa17 are all positive, which is a characteristic of helical secondary structures. Information about solvent accessibility of the exchangeable protons can be inferred from the temperature coefficients of the amide proton chemical shifts. Table I gives the observed values of these coefficients for every amino acid in the peptide. A lower temperature coefficient for an amide proton is usually indicative of some degree of protection from solvent. The standard values corresponding to highly exposed protons in unfolded structures were determined to be around 6×10^{-3} ppm/K (Deslauriers & Smith, 1980). With the exception of L1 and G17, the amide protons of Baa17 have temperature coefficients significantly lower than this value.

The pH value we used in our experiments was chosen to reproduce the physicochemical conditions under which CaM is stable and its backbone assignment was available (Ikura et al., 1990). Unfortunately, at this pH value the exchange kinetics of the amide protons in the free peptide are significantly increased, resulting in a relatively broad line width (compared to the coupling constant) and thus precluding a correct evaluation of accurate $J_{\alpha N}$ coupling constant. We have compared the 1D spectra of the free peptide at different concentrations between 0.5 and 6 mM. No significant changes of the amide proton line width were observed in this concentration range, indicating that the line broadening is not significantly determined by the molecular association.

CD Results. The CD spectra of 60 μM Baa17, in the same aqueous buffer, showed a significant negative ellipticity at 222 nm ($\theta_m = -10000$ deg cm^2 dmol^{-1}), a larger negative ellipticity at 204 nm ($\theta_m = -14000$ deg cm^2 dmol^{-1}) and a positive peak at 193 nm (data not shown), suggesting the presence of a small but significant population of helical secondary structure (Johnson, 1988). On addition of 6 M guanidinium chloride, a concentration which is high enough to prevent formation of any regular conformation, the band at 222 nm vanishes. Surprisingly, addition of increasing amounts of trifluoroethanol, a cosovent known to stabilize preexisting secondary conformations (Nelson & Kallenbach, 1986), had no significant effect on the CD spectra. Similar behavior has been recently described in a highly helical model peptide (Merutka et al., 1991). Using a simple algorithm (Chang et al., 1978) for the quantitative analysis of CD spectra, we estimated that the α-helix content is approximately 20% in aqueous buffer.

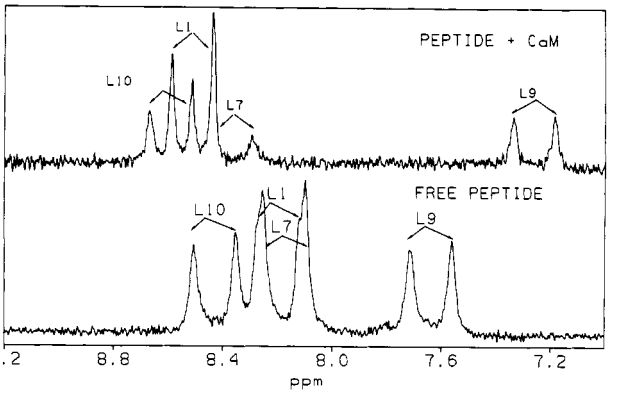

FIGURE 4: 600-MHz proton-detected ^{15}N-filtered 1D spectra obtained for Baa17 in a free state and bound to CaM. The 1:1 complex is 1.5 mM in a Bis-Tris buffer (20 mM), 6 mM $CaCl_2$, 100 mM KCl, and 5% ^2H_2O, at pH 6.3.

NMR Studies of the Bound Peptide

The 1D ^{15}N-filtered spectrum of an equimolar mixture of Baa17 and Ca^{2+}-saturated CaM (1.5 mM) is presented in Figure 4 and is compared with the corresponding filtered spectrum of the free peptide. Resonance assignment in the bound state will be presented later, in this paper. At a lower peptide/protein ratio the edited spectrum was identical, but the conventional 1D spectrum showed two distinct sets of resonances originating from the free and complexed CaM. This corresponds to a slow exchange on the NMR time scale between the two forms, as was already been described for a peptide derived from myosin light-chain kinase (Klevit et al., 1985; Ikura et al., 1991). Some information relevant to the bound state of the peptide could be inferred from Figure 4. The four doublets corresponding to the four ^{15}N-labeled Leu

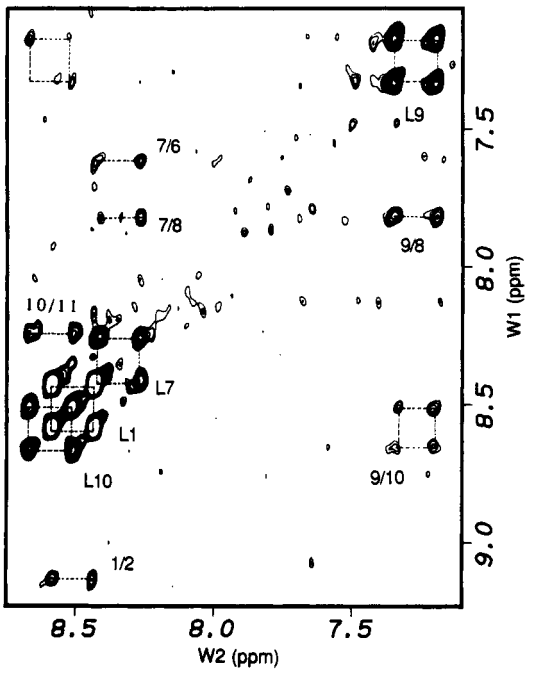

FIGURE 5: Portion of a 600-MHz $^{15}N(\omega_2)$-half-filtered NOESY spectrum of the Baa17/CaM complex (mixing time 100 ms) showing the amide/amide cross-peaks. The experimental conditions are the same as in Figure 4.

residues could be easily identified in the spectrum of the free peptide. One single set of four doublets are also visible in the bound state of the peptide, indicating that there is a single high-affinity binding site, in agreement with previous studies (DeGrado et al., 1985). The fact that all four doublets are significantly shifted in the complex is indicative of environmental and/or conformational changes upon complexation. In contrast with the free peptide, resonances in the bound state have variable line widths. One doublet has a line width comparable to that in the free state. This suggests that the broadening of the other resonances corresponds to site-specific immobilization rather than to exchange processes between multiple conformational states or binding sites.

$^{15}N(\omega_2)$-half-filtered NOESY and TOCSY experiments enabled us to obtain a partial assignment of the Baa17 spectrum in the peptide/CaM complex. Figure 5 shows a portion of the ω_2-filtered NOESY spectrum after 100 ms of mixing time. As is seen in the figure, all the ^{15}N-bound protons give strong NOE connectivities of comparable intensities with their neighboring amide protons. A careful analysis of this spectral region gave a consistent assignment for 8 out of 17 amide protons in the bound peptide. L9 and L10 give an NOE connectivity characteristic of consecutive labeled amide groups (Senn et al., 1987). The amide protons resonating at 7.26 and 8.32 ppm have NOE connectivities with the same proton resonating at 7.82 ppm. Therefore, the peak at 7.82 ppm should correspond to L8, the common neighbor of the labeled leucines L7 and L9. The remaining NOE cross-peaks allowed assignment of resonances coming from amide protons of L1, K2, L6, and K11. The CαH protons for L1, L9, and L10 were readily identified from the filtered TOCSY spectrum (not shown). The L7 amide proton resonance is too broad to give an observable NH/C_αH cross-peak. We were not able to observe the remote intrachain connectivities even at longer mixing times (up to 100 ms). The assigned resonances of the bound peptide are shown in parentheses in Table I. The ^{15}N resonances of the peptide (assigned from ^{15}N/H heteronuclear multiple-quantum correlation experiments) in the bound state are also considerably more dispersed than in the free state.

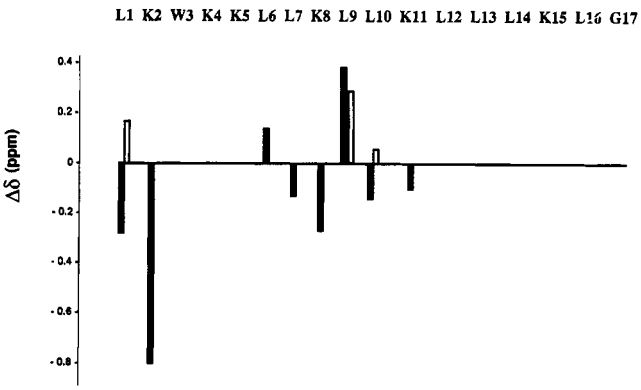

FIGURE 6: Histogram of the difference between the chemical shifts of free and CaM-bound Baa17 plotted against the primary structure. Only the NH (black sticks) and C_αH (empty sticks) assigned in both states are represented.

In particular, ^{15}N resonance of L7 is low-field shifted by about 2.5 ppm.

The analysis of the ω_2-filtered NOESY spectra also provides useful information on the conformational state of the bound peptide. All the sequential d_{NN} connectivities implicating the labeled residues were observed (Figure 5), and their integrals were found to have similar values. In addition, in contrast with the spectra of the free peptide, no $d_{\alpha N}(i,i+1)$ NOEs from the labeled amide groups were observed. Together, these two observations are highly indicative of an α-helix-type conformation (Wüthrich et al., 1984) spanning at least the L1–K11 fragment. From ^{15}N-filtered 1D spectra conducted at different temperatures between 278 and 310 K, we determined the temperature coefficients of the amide protons in the four labeled residues. In contrast with the high value for the N-terminal Leu (-8.0×10^{-3} ppm/K), L7 and L9 amide protons showed lower values than in the free state (-0.3×10^{-3} ppm/K).

Chemical shift changes of amide or C_α protons upon binding are also indicative of structural and/or environmental modifications. When possible, we calculated the difference between free and bound state chemical shifts. As is shown in Figure 6, all the assigned resonances of the peptide backbone change to various extents and in both directions. The three C_α resonances are all high-field shifted as expected for a stabilized helical structure. Changes of amide resonances are more sensitive to the state transformation but are less regular. Other factors, such as hydrogen-bond formation (Wagner et al., 1983) or ring current shifts induced by aromatic side chains, may be equally involved. For instance, the large low-field shift of the K2 amide resonance may be explained by the formation or strengthening of an intramolecular hydrogen bond and/or the deshielding effect of the W3 indole ring current. The opposite changes of K8 and L9 could be also partly determined by ring current shifts induced by aromatic residues of the protein.

Additional information characterizing the geometry and molecular contacts of the bound peptide was provided by the high-field region of the half-filtered NOESY spectrum of the complex (Figure 7). The L1 amide proton NOEs can be largely accounted for by intraresidue dipolar interactions; the string of cross-peaks of this proton is highly similar in the free and bound states. In contrast, the cross-peak patterns of the other ^{15}N-bound protons are significantly modified, indicating a change in side-chain conformation and magnetic environment. Furthermore, a number of new cross-peaks were observed, in particular in the high-field region of the spectrum, corresponding to ring current shifted resonances (boxed

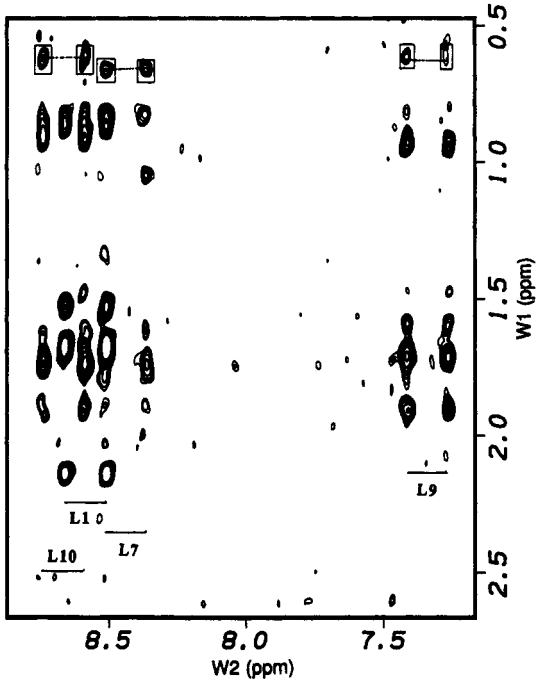

FIGURE 7: Portion of a 600-MHz $^{15}N(\omega_2)$-half-filtered NOESY (mixing time 250 ms) spectrum of the equimolar Baa17/CaM complex in the same experimental conditions as in Figure 4. The boxes indicate the cross-peaks not observed for Baa17 in the free state which correspond to ring current shifted protons.

cross-peaks in Figure 7). The high-field resonances may correspond to peptide or (more probably) protein protons in the neighboring of aromatic rings of CaM. In both cases this means that peptide region L7–L10 is close to aromatic residues of the CaM.

Discussion

A structural and dynamical description of Baa17/CaM interaction may provide a good model for better understanding of various intermolecular processes including substrate/enzyme, drug/receptor, or antigen/antibody reactions. The experiments presented here were mainly directed toward the characterization of the peptide itself both in free and complexed state, and our results are therefore complementary to those concerning the CaM features (Seeholzer & Wand, 1989; Ikura et al., 1991).

Free State Conformation. Several lines of NMR and CD experimental evidence indicate that in the free state Baa17 adopts an α-helical conformation which exchanges rapidly with unfolded conformations. The sequential distribution of strong d_{NN} and medium-range NOEs (Figure 3) allows us to identify the helix boundaries at W3 and L16. The preferred secondary conformation is stable enough to be detected at ambient temperature (298 K) and at a relatively high rate of amide proton exchange. Only few other short linear peptides have been shown to adopt a helical structure in aqueous solution (Kim & Baldwin, 1984; Schoemaker et al., 1985; Waltho et al., 1989).

Conformational Changes upon Binding. Changes in overall conformation and physicochemical environment of Baa17 upon complexation are reflected in a number of NMR parameters. The NOE patterns observed for the bound peptide are typical for an α-helix: relatively strong d_{NN} and absence of any $d_{\alpha N}$ connectivity (Wüthrich et al., 1984). As indicated by the edited 1D spectrum, we observed one single population of strongly bound peptide exploring a very narrow conformational space. Therefore, we can assume that upon binding to CaM the peptide conformational equilibrium is shifted toward a unique α-helical state. A similar conclusion was reached by indirect studies on the peptide/CaM complexes using CD or NMR methods. For instance, CD analysis showed that the negative ellipticity at 222 nm of the complex is larger than the sum of ellipticities of the isolated components, suggesting that the additional contribution is due to the increased helicity of the peptide (Cox et al., 1985; DeGrado et al., 1985; Garone & Steiner, 1990). The reasoning is, however, complicated by the fact that the CaM itself changes its conformation, as shown by small-angle X-ray and neutron diffraction (Heidorn et al., 1989; Trewhella et al., 1990) and NMR experiments (Seeholzer et al., 1986; Seeholzer & Wand, 1989; Ikura et al., 1991). Also, changes in CaM helicity were observed between crystal and solution states (Martin & Bayley, 1986) or were induced by the nonspecific action of helicogenic solvents (Bayley et al., 1988). The experimental approach presented here has the advantage of directly emphasizing the NMR parameters corresponding to the bound peptide only. The structural features based on our experiments confirm and complete the previous indirect observations.

Model of Interaction. General models aiming to explain the specificity of biochemical interactions between small molecules and proteins may consider either the preexistence of a stable structure of the ligand fitting exactly the shape of a rigid binding site ("lock and key") or a dynamic structural adjustment, during the interaction, of flexible ligand and receptor structures ("induced fit"). The present results may shed some light on this complex matter. A significant population of the free peptide exists in α-helical conformation which becomes the dominant conformation in the bound state. Observation of a strong $d_{NN}(1,2)$ connectivity in the bound state (Figure 6) but not in the free state (Figure 2) strongly suggests that the helical domain extends toward the N-terminal end of the peptide. Therefore, the intermolecular interactions select, stabilize, and extend a preexisting, moderately stable, secondary conformation of the peptide. Simultaneously, CaM itself undergoes detectable conformational changes in both globular domains (Seeholzer & Wand, 1989; Ikura et al., 1991).

The crystallographic studies revealed that CaM has a dumbbell shape consisting of two globular domains connected by a long helical linker (Babu et al., 1988). Each domain has two Ca^{2+}-binding sites (helix–loop–helix motifs) and a hydrophobic cleft which is thought to be the binding site for drugs or amphiphilic peptides.

A number of recent experiments were dedicated to the identification of the binding site in the CaM structure and characterization of the interaction geometry. From studies involving photoreactive Baa17 analogues, O'Neil and DeGrado (1989) suggested that the two ends of the peptide may interact simultaneously with the two different globular domains of CaM, which are brought closer than in the crystal structure by a disruption in the central helix. According to the model, the N- and C-terminal peptide fragments would interact more strongly and be more immobilized than the central fragment. This model is inconsistent with a number of feature of our present results.

The changes in chemical shifts of backbone protons (Figures 4 and 6) observed in the bound peptide (both highfield and lowfield relative to the free state) are difficult to explain by only the secondary structure modifications. For instance, the resultant secondary chemical shift of L9 amide proton (relative to the random coil) is about 1.2 ppm, three times larger than the average helix-type shift (0.40 ppm) (Szilagyi & Jardetzky,

1989). Therefore ring current contribution from CaM aromatic side chains may be taken into account. Existence of NOE connectivities between amide protons L7, L9, and L10 and ring current shifted protons (Figure 7) also indicates that the middle of the peptide sequence is situated in the vicinity of aromatic amino acids of CaM. However, the aromatic residues are distributed within the two hydrophobic domains and not in the central helix, which is mainly composed of charged residues. Thus, the present NMR data are indicative of an alternative complex model in which Baa17 interacts mainly with the hydrophobic patch of one single globular domain. A number of dynamical parameters measured in the present experiments are also consistent with this conclusion. Thus, the high temperature coefficient and the narrow amide resonance of L1 indicate that the N-terminal is not strongly implicated in intermolecular interactions. In contrast, the L7, L9, and L10 amide protons have a larger line width and a considerably decreased temperature coefficient, which is indicative of a high degree of immobilization and solvent protection.

Recent experimental or modeling data coming from different laboratories support the one domain interaction model. Thus, the isolated C-terminal domain of CaM was shown to preserve the capacity to bind different amphiphilic peptides (Garone & Steiner, 1990; Sanyal et al., 1988). Also, by analogy with crystallographic packing data of troponin C, Strynadka and James (1990) were able to build a plausible model for the interaction between mastoparan (a natural, 14 amino acid, amphiphilic peptide) and the C-terminal domain of CaM.

The extent and quality of the available experimental data could not eliminate the possibility of different interaction mechanisms, depending on the size and structure of the bound molecule. More structural data, at atomic level resolution, are needed to solve this problem. The approach presented here, applied to different labeled peptides, may provide a good experimental basis for a better understanding of the CaM/target interaction.

Acknowledgments

We thank J. Rosa for continuous support and W. Chazin, N. J. Skelton, and M. Rance for helpful discussions. Thanks are due to K. Soda for the kind gift of plasmid encoding L-leucine dehydrogenase from *Bacillus stearothermophilus* and to T. Rose, R. Sarfati, and O. Siffert for synthesis of ^{15}N-labeled peptide. We are indebted to J. Y. Lallemand, Ecole Polytechnique, Palaiseau, for the use of the NMR spectrometer and to E. Peter for carefully reading the manuscript.

Registry No. Baa17, 137232-24-7.

References

Babu, Y. S., Bugg, C. E., & Cook, W. J. (1988) *J. Mol. Biol. 204*, 191–204.

Bax, A., Griffey, R. H., & Hawkins, B. L. (1983) *J. Magn. Reson. 55*, 301–315.

Bayley, P., Martin, S., & Jones, G. (1988) *FEBS Lett. 238*, 61–66.

Chang, C. T., Wu, C.-S. C., & Yang, J. T. (1978) *Anal. Biochem. 91*, 13–31.

Cohen, P., & Klee, C. B., Eds. (1988) *Calmodulin. Molecular Aspects of Cellular Regulation*, Vol. 5, Elsevier Biomedical Press, Amsterdam.

Cox, J. A., Comte, M., Fitton, J. E., & DeGrado, W. F. (1985) *J. Biol. Chem. 260*, 2527–2534.

DeGrado, W. F., Prendergast, F. G., Wolfe, H. R., Jr., & Cox, J. A. (1985) *J. Cell. Biochem. 29*, 83–93.

Deslauriers, R., & Smith, I. C. P. (1980) *Biol. Magn. Reson. 2*, 243–344.

Eich, G., Bodenhausen, G., & Ernst, R. R. (1982) *J. Am. Chem. Soc. 104*, 3731–3732.

Fesik, S. W., & Zuiderweg, E. R. P. (1990) *Q. Rev. Biophys. 23*, 97–131.

Garone, L., & Steiner, R. F. (1990) *Arch. Biochem. Biophys. 276*, 12–18.

Hancock, W. S., Prescott, D. J., Vagelos, P. R., & Marshall, G. R. (1973) *J. Org. Chem. 38*, 774–781.

Heidorn, D. B., Seeger, P. A., Rokop, S. E., Blumenthal, D. K., Means, A. R., Crespi, H., & Trewhella, J. (1989) *Biochemistry 28*, 6757–6764.

Ikura, M., Kay, L. E., & Bax, A. (1990) *Biochemistry 29*, 4659–4667.

Ikura, M., Kay, L. E., Krinks, M., & Bax, A. (1991) *Biochemistry 30*, 5498–5504.

Jeener, J., Meier, B. H., Bachmann, P., & Ernst, R. R. (1979) *J. Chem. Phys. 71*, 4546–4553.

Johnson, W. C., Jr. (1988) *Annu. Rev. Biophys. Biophys. Chem. 17*, 145–166.

Kim, P. S., & Baldwin, R. L. (1984) *Nature (London) 307*, 329–334.

Klevit, R. E., Blumenthal, D. K., Wemmer, D. E., & Krebs, E. G. (1985) *Biochemistry 24*, 8152–8157.

Martin, S. R., & Bayley, P. M. (1986) *Biochem. J. 238*, 485–490.

Merutka, G., Shalongo, W., & Stellwagen, E. (1991) *Biochemistry 30*, 4245–4248.

Mocanu, A., Niac, G., Ivanof, A., Gorun, V., Palibroda, N., Vargha, E., Bologa, M., & Bârzu, O. (1982) *FEBS Lett. 143*, 153–156.

Nagata, S., Tanizawa, K., Esaki, N., Sakamoto, Y., Ohshima, T., Tanaka, H., & Soda, K. (1988) *Biochemistry 27*, 9056–9062.

Nelson, J. W., & Kallenbach, N. R. (1986) *Proteins 1*, 211–217.

O'Neil, K. T., & DeGrado, W. F. (1989) *Proteins 6*, 284–293.

O'Neil, K. T., & DeGrado, W. F. (1990) *Trends Biochem. Sci. 15*, 59–64.

O'Neil, K. T., Wolfe, H. R., Jr., Erickson-Viitanen, S., & DeGrado, W. F. (1987) *Science 236*, 1454–1456.

O'Neil, K. T., Erickson-Viitanen, S., & DeGrado, W. F. (1989) *J. Biol. Chem. 264*, 14571–14578.

Otting, G., & Wüthrich, K. (1990) *Q. Rev. Biophys. 23*, 39–96.

Rance, M. (1987) *J. Magn. Reson. 74*, 557–564.

Rance, M., Sorensen, O. W., Bodenhausen, G., Wagner, G., Ernst, R. R., & Wüthrich, K. (1983) *Biochem. Biophys. Res. Commun. 117*, 479–485.

Sanyal, G., Richard, L. M., Carraway, K. L., & Puett, D. (1988) *Biochemistry 27*, 6229–6236.

Schoemaker, K. R., Kim, P. S., Brems, D. N., Marqusee, S., York, E. J., Chaiken, I. M., Stewart, J. M., & Baldwin, R. L. (1985) *Proc. Natl. Acad. Sci. U.S.A. 82*, 2349–2353.

Seeholzer, S. H., & Wand, A. J. (1989) *Biochemistry 28*, 4011–4020.

Seeholzer, S. H., Cohn, M., Putkey, J. A., Means, A. R., & Crespi, H. L. (1986) *Proc. Natl. Acad. Sci. U.S.A. 83*, 3634–3638.

Senn, H., Eugster, A., Otting, G., Suter, F., & Wüthrich, K. (1987) *Eur. Biophys. J. 14*, 301–306.

Strynadka, N. C. J., & James, M. N. G. (1990) *Proteins 7*, 234–248.

Szilagyi, L., & Jardetzky, O. (1989) *J. Magn. Reson. 83*, 441-449.
Trewhella, T., Blumenthal, D. K., Rokop, S. E., & Seeger, P. A. (1990) *Biochemistry 29*, 9316-9324.
Veitch, N. C., Concar, D. W., Williams, R. J. P., & Whitford, D. (1988) *FEBS Lett. 238*, 49-55.
Wagner, G., Pardi, A., & Wüthrich, K. (1983) *J. Am. Chem. Soc. 105*, 5948-5949.
Waltho, J. P., Feher, V. A., Lerner, R. A., & Wright, P. E. (1989) *FEBS Lett. 250*, 400-404.
Wright, P. E., Dyson, H. J., & Lerner, R. A. (1988) *Biochemistry 27*, 7167-7175.
Wüthrich, K. (1986) *NMR of Proteins and Nucleic Acids*, John Wiley and Sons, New York.
Wüthrich, K., Billeter, M., & Brown, W. (1984) *J. Mol. Biol. 180*, 715-740.

Solution Structure of Murine Epidermal Growth Factor Determined by NMR Spectroscopy and Refined by Energy Minimization with Restraints[†,‡]

Gaetano T. Montelione,[§] Kurt Wüthrich,[∥] Antony W. Burgess,[⊥] Edward C. Nice,[⊥] Gerhard Wagner,[#] Kenneth D. Gibson,[▽] and Harold A. Scheraga*[,▽]

Center for Advanced Biotechnology and Medicine, and Department of Chemistry, Rutgers University, Piscataway, New Jersey 08854-5635, Institut für Molekularbiologie und Biophysik, Eidenössische Technische Hochschule-Hönggerberg, CH-8093 Zürich, Switzerland, Ludwig Institute for Cancer Research, Melbourne Tumour Biology Branch, Victoria 3050, Australia, Department of Biological Chemistry and Molecular Pharmacology, Harvard University, 240 Longwood Avenue, Boston, Massachusetts 02115, and Baker Laboratory of Chemistry, Cornell University, Ithaca, New York 14853-1301

Received June 4, 1991; Revised Manuscript Received September 18, 1991

ABSTRACT: The solution structure of murine epidermal growth factor (mEGF) at pH 3.1 and a temperature of 28 °C has been determined from NMR data, using distance geometry calculations and restrained energy minimization. The structure determination is based on 730 conformational constraints derived from NMR data, including 644 NOE-derived upper bound distance constraints, constraints on the ranges of 32 dihedral angles based on measurements of vicinal coupling constants, and 54 upper and lower bound constraints associated with nine hydrogen bonds and the three disulfide bonds. The distance geometry interpretation of the NMR data is based on previously published sequence-specific ^{1}H resonance assignments [Montelione et al. (1988) *Biochemistry 27*, 2235-2243], supplemented here with individual assignments for some side-chain amide, methylene, and isopropyl methyl protons. The molecular architecture of mEGF is the same as that described previously [Montelione et al. (1987) *Proc. Natl. Acad. Sci. U.S.A. 84*, 5226-5230], but the structure is overall more precisely determined by a more extensive set of NMR constraints. Analysis of proton NMR line widths, amide proton exchange rates, and side-chain $^3J(H^{\alpha}-H^{\beta})$ coupling constants provides evidence for internal motion in several regions of the mEGF molecule. Because mEGF is one member of a large family of homologous growth factors and protein domains for which X-ray crystal structures are not yet available, the atomic coordinates resulting from the present structure refinement (which we have deposited in the Brookhaven Protein Data Bank) are important data for understanding the structures of EGF-like proteins and for further detailed comparisons of these structures with mEGF.

Epidermal growth factor (EGF)[1] is a small mitogenic protein containing 53 amino acids and three disulfide bonds (Cohen, 1962; Savage et al., 1972, 1973). EGF and EGF-like proteins are thought to play important roles in wound healing (Burgess, 1989) and oncogenesis (Sporn & Todaro, 1980; Sporn & Roberts, 1985; Heldin & Westermark, 1990). Although no crystal structure is available for EGF, or for any proteins homologous to EGF, solution structures derived from NMR measurements are available for human EGF (Carver et al., 1986; Cooke et al., 1987), murine EGF (Montelione et al., 1986, 1987; Kohda & Inagaki, 1988; Kohda et al., 1988), and rat EGF (Mayo et al., 1989), as well as for the homologous human type α transforming growth factor (TGFα)

[†] This work was supported by research grants from the National Institute of General Medical Sciences (GM-24893), the American Cancer Society, the Schweizerischer Nationalfonds (project 3.198.85), the Damon Runyon Walter Winchell Cancer Research Foundation (DRG-920), and the Searle Scholars Progam/The Chicago Community Trust. Support was also received from the National Foundation for Cancer Research.

[‡] The atomic coordinates have been deposited in the Brookhaven Protein Data Bank.

* Author to whom correspondence should be addressed.
[§] Rutgers University.
[∥] Institute für Molekularbiologie und Biophysik.
[⊥] Ludwig Institute for Cancer Research.
[#] Harvard University.
[▽] Cornell University.

[1] Abbreviations: EGF, epidermal growth factor; mEGF, murine EGF; hEGF, human EGF; TGF-α, type α transforming growth factor; hTGFα, human TGFα; 2D, two dimensional; COSY, 2D correlated spectroscopy; 2QF-COSY, 2D two-quantum filtered COSY; COSY-30, COSY in which the mixing pulse has a 30° flip angle; DISMAN, program used to calculate molecular structures from internuclear distance constraints; E-COSY, 2D exclusive COSY; NOE, nuclear Overhauser effect; NOESY, 2D NOE spectroscopy; RMSD, root-mean-square deviation; ECEPP/2, empirical conformational energy program for peptides.

0006-2960/92/0431-236$03.00/0